

## Proton Diffusion at Phospholipid Assemblies

Jie Zhang and Patrick R. Unwin\*

*Contribution from the Department of Chemistry, University of Warwick, Coventry CV4 7AL, UK*

Received August 30, 2001

**Abstract:** A new scanning electrochemical microscopy proton feedback method has been developed for investigating lateral proton diffusion at phospholipid assemblies: specifically Langmuir monolayers at the water/air interface. In this approach, a base is electrogenerated by the reduction of a weak acid (producing hydrogen) at a "submarine" ultramicroelectrode (UME) placed in the aqueous subphase of a Langmuir trough close to a monolayer. The electrogenerated base diffuses to and titrates monolayer-bound protons and is converted back to its initial form, so enhancing the current response at the UME. Local deprotonation of the monolayer creates a concentration gradient for lateral proton diffusion. A numerical model has been developed, taking into account the potential-dependent association/dissociation constant of the interfacial acid groups. A comparison is made of monolayers comprising either acidic DL- $\alpha$ -phosphatidyl-L-serine, dipalmitoyl (DPPS) or zwitterionic L- $\alpha$ -phosphatidylcholine, dipalmitoyl (DPPC) monolayers at a range of surface pressures. It is demonstrated that lateral proton fluxes at DPPS are significant, but the lateral proton diffusion coefficient is lower than in bulk solution. In contrast, lateral proton diffusion cannot be detected at DPPC, suggesting that the acid/base character of the phospholipid is important in determining the magnitude of interfacial proton fluxes.

## Introduction

Proton conduction is important in a wide range of areas, including photosynthesis in green plants, the production of electricity in hydrogen fuel cells, electrochemical sensors, electrochemical reactors, and electrochromic devices.<sup>1</sup> In biological systems, proton migration between source and sink sites is a key step in bioenergetic processes in cellular membranes.<sup>2-7</sup> Such processes are controlled by pH gradients, which couple, for example, electron transfer and ATP synthesis in mitochondria, chloroplasts, and bacteria.<sup>2</sup> Lateral diffusion has been proposed as a mechanism for proton transport,<sup>3,4</sup> but it has proved difficult to measure the rate of this process with conventional techniques.<sup>5-10</sup>

Langmuir monolayers of phospholipids at the water/air (W/A) interface are attractive models for physicochemical studies of cellular membranes, because the composition of these self-assembled systems is readily controlled and varied.<sup>2</sup> Lateral proton diffusion in monolayers has previously been investigated

by time-of-flight fluorescence measurements<sup>3,10,11</sup> and conductivity<sup>12</sup> over centimeter length scales. Facilitated lateral proton conductance has been advocated for pure phospholipids (both zwitterionic and acidic), phospholipid mixtures, and pure protein monolayers.<sup>3,11</sup> In contrast, laser pulse measurements of proton dwell times in vesicles have found no evidence for unusually high lateral proton mobility.<sup>13</sup>

Scanning electrochemical microscopy (SECM)<sup>9,14-16</sup> allows interfacial dynamics and diffusion to be studied on small length and time scales approaching those relevant to cellular membranes. In recent applications to assemblies at the W/A interface, SECM has been used to study lateral proton diffusion along a stearic acid monolayer,<sup>9</sup> the effect of a 1-octadecanol monolayer on oxygen transfer across the W/A interface,<sup>17</sup> and lateral conductivity in assemblies of metal nanoparticles.<sup>18</sup> In these

\* Address correspondence to this author. E-mail: p.r.unwin@warwick.ac.uk.

- (1) Kreuer, K. D. *Chem. Mater.* **1996**, *8*, 610.
- (2) Gennis, R. B. *Biomembranes: Molecular Structure and Function*; Springer-Verlag: New York, 1989.
- (3) Teissié, J.; Gabriel, B.; Prats, M. *Trends Biochem. Sci.* **1993**, *18*, 243.
- (4) Kell, D. B. *Biochim. Biophys. Acta* **1979**, *549*, 55.
- (5) Scherrer, P. *Nature* **1995**, *374*, 222.
- (6) Alexiev, U.; Scherrer, P.; Mollaaghhaba, R.; Khornaa, H. G.; Heyn, M. P. *Proc. Natl. Acad. Sci. U.S.A.* **1995**, *92*, 372.
- (7) Heberle, J.; Riesle, J.; Thiedemann, G.; Oesterhelt, D.; Dencher, N. A. *Nature* **1994**, *370*, 379.
- (8) (a) Teissié, J. *Nature* **1996**, *379*, 305. (b) Scherrer, P. *Nature* **1996**, *379*, 306.
- (9) Slevin, C. J.; Unwin, P. R. *J. Am. Chem. Soc.* **2000**, *122*, 2597 and references therein.
- (10) Teissié, J.; Prats, M.; Soucaille, P.; Tocanne, F. *Proc. Natl. Acad. Sci. U.S.A.* **1985**, *82*, 3217.
- (11) (a) Gabriel, B.; Teissié, J. *Proc. Natl. Acad. Sci. U.S.A.* **1996**, *93*, 14521. (b) Prats, M.; Teissié, J.; Tocanne, F. *Nature* **1986**, *322*, 756. (c) Gabriel B.; Teissié J. *J. Am. Chem. Soc.* **1991**, *113*, 8818.
- (12) Leite, V. B. P.; Cavalli, A.; Oliveira, O. N., Jr. *Phys. Rev. E* **1998**, *57*, 6835.
- (13) (a) Gutman, M.; Nachliel E. *Biochim. Biophys. Acta* **1995**, *1231*, 123. (b) Nachliel, E.; Gutman, M. *J. Am. Chem. Soc.* **1988**, *110*, 2629.
- (14) Bard, A. J.; Fan F. R.-F.; Kwak, J.; Lev, O. *Anal. Chem.* **1989**, *61*, 132.
- (15) See for example: (a) Tsionsky, M.; Bard, A. J.; Mirkin, M. V. *J. Am. Chem. Soc.* **1997**, *119*, 10785. (b) Mirkin, M. V.; Fan, F. R.-F.; Bard, A. J. *Science* **1992**, *257*, 364. (c) Fan, F. R.-F.; Bard, A. J. *Science* **1997**, *267*, 871. (d) Gonsalves, M.; Barker, A. L.; Macpherson, J. V.; Unwin, P. R.; O'Hare, D.; Winlove, C. P. *Biophys. J.* **2000**, *78*, 1578. (e) Liu, B.; Rotenberg, S. A.; Mirkin, M. V. *Proc. Natl. Acad. Sci. U.S.A.* **2000**, *97*, 9855. (f) Basame, S. B.; White, H. S. *J. Phys. Chem. B* **1998**, *102*, 9812. (g) Uitto, O. D.; White, H. S. *Anal. Chem.* **2001**, *73*, 533.
- (16) See for example: (a) *Scanning Electrochemical Microscopy*; Bard, A. J., Mirkin, M. V., Eds.; Marcel Dekker: New York, 2001. (b) Barker, A. L.; Slevin, C. J.; Unwin, P. R.; Zhang, J. In *Liquid Interfaces in Chemical, Biological and Pharmaceutical Applications*; Volkov, A. G., Ed.; Marcel Dekker: New York, 2001; p 283.
- (17) Slevin, C. J.; Ryley, S.; Walton, D. J.; Unwin, P. R. *Langmuir* **1998**, *14*, 5331.

studies, the response of a probe ultramicroelectrode (UME) either translated toward or held close to a spot at a target interface was used to obtain quantitative data on a local scale.

The feedback mode<sup>16</sup> is one of the most popular SECM methods, but at present is based mainly on redox mediators. This paper reports investigations of lateral proton diffusion processes in phospholipid assemblies under well-posed conditions, with a new SECM proton feedback method that utilizes a weak acid/base couple. The proposed approach allows processes to be investigated under more physiologically relevant pH conditions, compared to an earlier SECM induced desorption technique.<sup>9</sup> Moreover, the use of a weak acid as a proton carrier, rather than the free proton, significantly decreases the diffusion coefficient of the proton source in the solution phase, so that the contribution of lateral proton diffusion to the UME tip response becomes more pronounced. Here, quantitative studies demonstrate, for the first time, that lateral proton fluxes in acidic phospholipids are significant, but the associated lateral proton diffusion coefficient is much lower than that in bulk solution.

## Experimental Section

**Chemicals.** All chemicals were used as received. They were DL- $\alpha$ -phosphatidyl-L-serine, dipalmitoyl (DPPS, 98%, Sigma-Aldrich), L- $\alpha$ -phosphatidylcholine, dipalmitoyl (DPPC, 99+%, Sigma-Aldrich),  $\text{KH}_2\text{PO}_4$  (AnalaR, BDH), tetramethylammonium chloride (TMACl) (>98%, Fluka), and chloroform (HPLC grade, BDH). All aqueous solutions were prepared from Milli-Q reagent water (Millipore Corp.).

**Apparatus.** The Langmuir trough (model 611, Nima Technology, Coventry, UK) was housed inside a purgebox (Glovebox Technology, Huntingdon, UK). Monolayers were observed using a Brewster angle microscope (MiniBAM, Nanofilm Technologie GmbH, Göttingen, Germany). The electrode was positioned using a set of  $x,y,z$  stages (M-462, Newport Corp., CA) and a piezoelectric positioner and controller (models P843.30 and E662, Physik Instrumente, Waldbronn, Germany). The procedure for the fabrication of "submarine" UMEs has been described previously.<sup>17,19</sup> The platinum UME used was a 25  $\mu\text{m}$  diameter disk electrode with a glass insulating sheath, characterized by an RG value<sup>20</sup> (overall probe radius to the electrode radius) of 10.

**Procedures.** Monolayers of phospholipids were formed by spreading a known volume of a chloroform solution containing 1 mM phospholipid to the aqueous subphase, typically comprising 1 mM  $\text{KH}_2\text{PO}_4$  and 0.05 M tetramethylammonium chloride (TMACl) electrolyte, using a microliter syringe (100  $\mu\text{L}$  volume, Hamilton, Reno, NV). The solvent was allowed to evaporate for 15 min before any measurements were made. Pressure–area isotherms were recorded with a barrier speed of 25  $\text{cm}^2 \text{min}^{-1}$ , from an initial surface area of 500  $\text{cm}^2$ .

Electrochemical measurements were made with use of a two-electrode arrangement, with the submarine UME as the working electrode and a silver wire as a quasi-reference electrode (AgQRE). The potential of the UME was controlled by using a purpose-built voltage generator and currents measured with a current follower. Current–time transients and current–distance approach curves were recorded directly to a PC with use of a data acquisition card (Lab-PC-1200, National Instruments, Austin, TX).

For SECM studies of phospholipid monolayers, the submarine UME was positioned in the aqueous subphase in a Langmuir trough, at a small distance,  $d$ , below a monolayer (Figure 1). The UME was used to generate a base ( $\text{HPO}_4^{2-}$ ) by electroreduction of a weak acid ( $\text{H}_2\text{PO}_4^-$ ) present in the solution. The base could diffuse to the

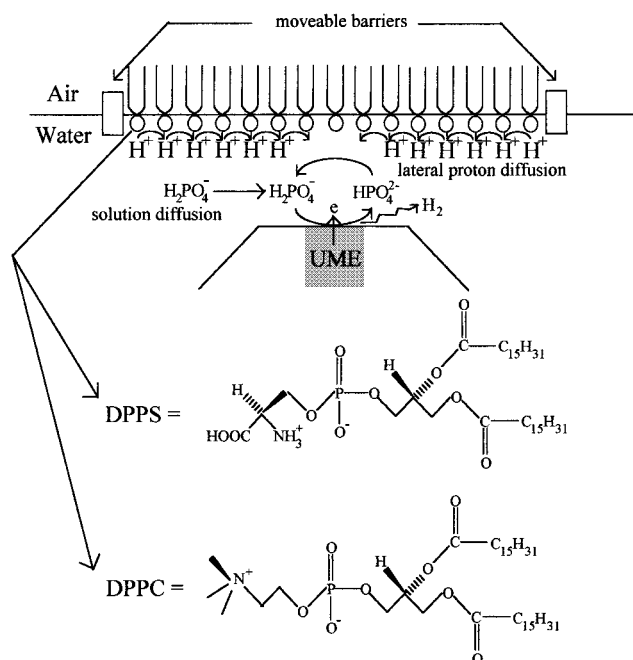


**Figure 1.** Schematic of steady-state SECM proton feedback measurements of lateral diffusion in phospholipid monolayers (not to scale).

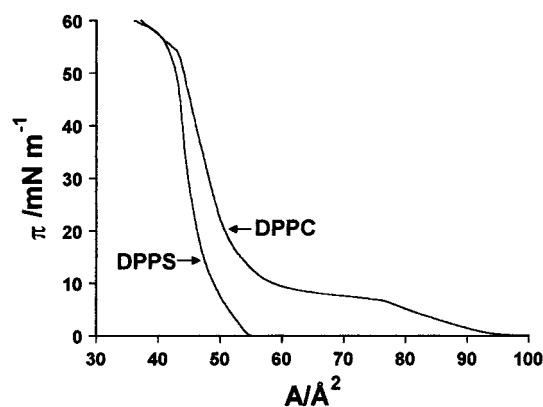


**Figure 2.** Pressure–area isotherms for DPPS and DPPC on an aqueous subphase containing 1 mM  $\text{KH}_2\text{PO}_4$  and 0.05 M TMACl.

monolayer and titrate away locally bound protons, producing  $\text{H}_2\text{PO}_4^-$  which diffused back to the electrode, undergoing further electron transfer. Provided that the initial density of protons at the monolayer is significant, the electrochemical depletion of surface-bound protons in a localized spot generates a radial interfacial proton flux that is ultimately detected as a current flow at the UME tip.

All electrochemical measurements were made under an Ar atmosphere in a temperature-controlled environment ( $23 \pm 0.5$   $^\circ\text{C}$ ).

## Results and Discussion

**Pressure–Area Isotherm Measurements.** Isotherms of surface pressure ( $\pi$ ) versus area per phospholipid molecule ( $A$ ) for the two monolayers, on an aqueous subphase of 1 mM  $\text{KH}_2\text{PO}_4$  and 0.05 M TMACl, are shown in Figure 2. The cation of this electrolyte has little binding affinity for the phospholipids over the pH range of the SECM studies.<sup>21</sup> The isotherm for the DPPC monolayer showed characteristic phases:<sup>22–24</sup> gaseous

(18) Quinn, B. M.; Prieto, I.; Haram, S. K.; Bard, A. J. *J. Phys. Chem. B* **2001**, *105*, 7474.

(19) Slevin, C. J.; Umbers, J. A.; Atherton, J. H.; Unwin, P. R. *J. Chem. Soc., Faraday Trans.* **1996**, *92*, 5177.

(20) Kwak, J.; Bard, A. J. *Anal. Chem.* **1989**, *61*, 1221.

(21) Tsui, F. C.; Ojcius, D. M.; Hubbell, W. L. *Biophys. J.* **1986**, *49*, 459.

(22) Ravaine, S.; Fanucci, G. E.; Seip, C. T.; Adair, J. H.; Talham, D. R. *Langmuir* **1998**, *14*, 708.

(23) Koyanova, R.; Caffrey, M. *Biochim. Biophys. Acta* **1998**, *1376*, 91.

(24) Mitchell, M. L.; Dluhy, R. A. *J. Am. Chem. Soc.* **1988**, *110*, 712.

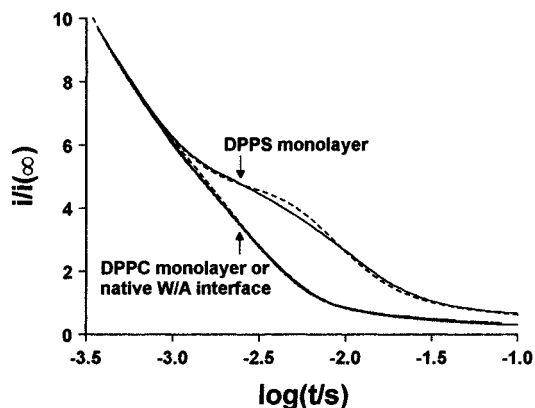


**Figure 3.** Current as a function of time,  $t$ , for the reduction of 1 mM  $\text{H}_2\text{PO}_4^-$  at an UME, positioned at  $d = 2.5 \mu\text{m}$  from a DPPS monolayer ( $\pi = 6 \text{ mN m}^{-1}$ ), a DPPC monolayer ( $\pi = 22 \text{ mN m}^{-1}$ ), or a native W/A interface. The experimental data are shown as solid lines and the dashed lines are theory for either protonation/deprotonation with the parameters in the text (DPPS case) or an inert interface (DPPC monolayer or native W/A interface).

phase ( $A > 100 \text{ \AA}^2$ ), liquid-expanded phase ( $100 \text{ \AA}^2 > A > 77 \text{ \AA}^2$ ), and liquid-expanded phase to liquid-condensed phase transition (plateau region), ultimately forming a liquid-condensed phase at small  $A$  values. In contrast, the isotherm for DPPS showed a phase transition (at  $A = 55 \text{ \AA}^2$ ) from the gaseous/liquid-expanded coexistence phase to a liquid-condensed phase, in agreement with previous studies.<sup>22,25</sup> BAM measurements demonstrated that monolayers were uniform over a wide range of  $A$  values of interest in the present studies.

**SECM Transient Measurements.** For transient experiments, the UME tip was positioned at a distance ( $d$ ) of  $2.5 \mu\text{m}$  from the monolayer surface. The potential was switched from a value where there was no electrochemical process to one where  $\text{H}_2\text{PO}_4^-$  was reduced to  $\text{HPO}_4^{2-}$  at a diffusion-controlled rate. A potential of  $-0.83 \text{ V}$  vs AgQRE was required to effect the diffusion-limited reduction of  $\text{H}_2\text{PO}_4^-$ , as determined by steady-state voltammetry. These latter measurements also showed that  $\text{H}_2\text{PO}_4^-$  was the predominant species in solution at the initial pH of ca. 5.2.

The transient current provided information on the diffusion of  $\text{H}_2\text{PO}_4^-$  to the UME and the titration of acid functionalities in the monolayer by electrogenerated  $\text{HPO}_4^{2-}$ . The distance was established by measuring the long time (steady-state) current, which was matched to steady-state approach curves, as reported in the next section. With care, this method allowed distances to be determined with a precision of  $\pm 0.2 \mu\text{m}$  for a typical tip/monolayer separation of  $2.5 \mu\text{m}$ , which had only a minor effect on the simulated transient. Typical transient results (Figure 3) showed that the current,  $i$ , normalized with respect to the steady-state bulk current for  $\text{H}_2\text{PO}_4^-$  reduction,  $i(\infty)$ , was significantly larger when the UME tip was positioned beneath a DPPS monolayer, compared to either a native W/A interface or one covered by a monolayer of DPPC. The additional current can be assigned to deprotonation of DPPS by  $\text{HPO}_4^{2-}$ , forming  $\text{H}_2\text{PO}_4^-$  that is detected at the UME. The driving force for interfacial proton transfer<sup>26</sup> from the monolayer to  $\text{HPO}_4^{2-}$  is high due to the large difference in the  $\text{p}K'_a$  of  $\text{H}_2\text{PO}_4^-$  (ca. 7.1) and the carboxylic group of DPPS (intrinsic  $\text{p}K'_a$  ca. 3.6).<sup>21</sup>

Because of interfacial potential effects at the phospholipid monolayer, discussed below, there is a sizable surface concentration of protons to be detected in this measurement, even though the initial pH is significantly higher than  $\text{p}K'_a$ . Only a background signal due to solution diffusion of  $\text{H}_2\text{PO}_4^-$  to the UME was observed for the DPPC monolayer, because it was zwitterionic throughout the experimental conditions herein.

Quantitative insight into the deprotonation process for the DPPS monolayer was obtained by modeling the time-dependent diffusion of  $\text{H}_2\text{PO}_4^-$  and  $\text{HPO}_4^{2-}$ .<sup>9</sup> Although  $\text{H}_2\text{PO}_4^-$  is reduced via dissociation and electron transfer to the free proton,<sup>27</sup> the deprotonation step was found to be nonlimiting, so that the usual SECM diffusion equation<sup>28</sup> applied:

$$\frac{\partial c}{\partial t} = D_{\text{sol}} \left( \frac{\partial^2 c}{\partial r^2} + \frac{1}{r} \frac{\partial c}{\partial r} + \frac{\partial^2 c}{\partial z^2} \right) \quad (1)$$

where  $c$  and  $D_{\text{sol}}$  are the concentration and diffusion coefficient of  $\text{H}_2\text{PO}_4^-$  in solution,  $r$  and  $z$  are axisymmetric cylindrical coordinates defining the SECM geometry in the radial and normal directions relative to the electrode surface, starting at its center, and  $t$  is time.

For the lateral proton diffusion process along the monolayer, the following equation is considered:

$$\frac{\partial \theta}{\partial t} = D_{\text{lat}} \left( \frac{\partial^2 \theta}{\partial r^2} + \frac{1}{r^2} \frac{\partial \theta}{\partial r} \right) \quad (2)$$

where  $\theta$  is the surface coverage of protonated amphiphilic moieties and  $D_{\text{lat}}$  is the lateral diffusion coefficient of the proton at the interface. In principle, the lateral diffusion of phospholipid amphiphile is also possible, but this is much slower<sup>29</sup> and so can be neglected.

For rapid acid/base processes (on the SECM time scale), the concentrations of  $\text{H}_2\text{PO}_4^-$  and  $\text{HPO}_4^{2-}$  at the monolayer interface can be related to the acid dissociation constant of the carboxylic acid group of DPPS,  $K_a$ , the fraction of protonated acidic groups,  $\theta$ , and the dissociation constant of  $\text{H}_2\text{PO}_4^-$ ,  $K'_a$ :

$$\frac{K_a}{K'_a} = \frac{c_{\text{int}}(1 - \theta)}{(c^* - c_{\text{int}})\theta} \quad (3)$$

where  $c^*$  is the total bulk concentration of phosphate moieties (weak acid and base) and  $c_{\text{int}}$  is the interfacial concentration of  $\text{H}_2\text{PO}_4^-$ . This equation is derived assuming a mass balance for phosphate at any point in space. To solve the problem numerically, the usual initial conditions and boundary conditions for SECM apply.<sup>28</sup> The following interfacial mass balance can be used in conjunction with eq 3 to ensure the conservation of protons:

$$\Gamma \int_{\theta_1}^{\theta_2} d\theta = \int_{d-\Delta z}^d dc(z) dz \quad (4)$$

where  $\Gamma$  is the surface concentration of amphiphile (determined by the surface pressure) and  $\theta_1$  and  $\theta_2$  are limits on the proton surface coverage that cause a change in the concentration of  $\text{H}_2\text{PO}_4^-$  close to the monolayer (located at  $z = d$ ) over a small distance,  $\Delta z$ .

(25) Minones, J.; Conde, O. *Colloid Polym. Sci.* **1988**, *266*, 353.

(26) Marcus, R. A. *Faraday Discuss. Chem. Soc.* **1982**, *74*, 7.

(27) Albery, W. J. *Electrode Kinetics*; Clarendon Press: Oxford, 1975.

(28) Unwin, P. R.; Bard, A. J. *J. Phys. Chem.* **1991**, *95*, 7814.

(29) Adalsteinsson, T.; Yu, H. *Langmuir* **2000**, *16*, 9410.

$K_a$  in eq 3 is surface potential dependent,<sup>9,30</sup> and is related to the intrinsic acid dissociation constant,  $K_a^i$ , by

$$K_a = K_a^i \exp(F\psi_0/RT) \quad (5)$$

where  $\psi_0$  is the surface potential,  $F$  is Faraday's constant, and  $R$  and  $T$  are the gas constant and absolute temperature. The surface potential–charge density relationship was calculated by using the Gouy–Chapman model,<sup>9,21,31</sup>

$$\sigma_0 = (8\epsilon\epsilon_0 c_{se}^*)^{1/2} \sinh(F\psi_0/2RT) \quad (6)$$

where  $\sigma_0$  is the charge density;  $\epsilon$  is the dielectric constant at the interface, which is ca. 30 for lipid monolayers,<sup>32,33</sup>  $\epsilon_0$  is the permittivity of free space, and  $c_{se}^*$  is the bulk concentration of the (1:1) supporting electrolyte. The negative charge that develops at the interface due to deprotonation of the carboxylic acid group in DPPS, by  $\text{HPO}_4^{2-}$ , defines the surface charge density,

$$\sigma_0 = F(\theta - 1)\Gamma \quad (7)$$

Under initial conditions with  $\Gamma = 3.3 \times 10^{-10} \text{ mol cm}^{-2}$  ( $A = 50 \text{ \AA}^2$ ) and  $c_{se}^* = 0.02 \text{ M}$ , eqs 3 and 5–7 predict  $\theta = 0.80$  and  $\text{p}K_a = 5.80$ . This confirms that there are sufficient surface-bound protons for the feedback measurement. It is important to emphasize that eqs 5–7 imply that the apparent  $\text{p}K_a$  will increase further as deprotonation occurs during the course of a transient measurement. These chemical processes were solved within the standard SECM diffusion model,<sup>9,34,35</sup> to obtain the time-dependent tip current at a specific tip/monolayer separation, after suddenly jumping the potential to cause the diffusion-limited reduction of  $\text{H}_2\text{PO}_4^-$ . The local boundary concentration of  $\text{H}_2\text{PO}_4^-$  was updated by using eqs 3–7, in an iterative fashion for each time-step increment, so that a protonation equilibrium prevailed at the interface, as defined by eq 3.

The experimental transient response of the UME for the DPPS monolayer matches well to the theoretical prediction, using the known  $\text{p}K_a'$  and  $\text{p}K_a^i$  values cited above, confirming the validity of the model. The short time transient response is insensitive to lateral diffusion and is governed solely by deprotonation of the monolayer and diffusion of  $\text{H}_2\text{PO}_4^-$  in solution.<sup>34</sup>

**Steady-State SECM Measurements.** Lateral proton diffusion was investigated by steady-state approach curves,<sup>9,14a</sup> since surface diffusion contributes primarily to the long-time SECM current response.<sup>34</sup> Approach curves were obtained by slowly translating the UME probe (at  $0.5 \mu\text{m/s}$ ) toward the interface and measuring the current for the reduction of  $0.5 \text{ mM H}_2\text{PO}_4^-$  as a function of  $d$ . Typical results in Figure 4a indicated an enhanced reduction current for the probe approaching the DPPS monolayer. This can be attributed to lateral proton diffusion providing an additional proton source, which is detected by SECM proton feedback mediated through  $\text{H}_2\text{PO}_4^-/\text{HPO}_4^{2-}$ . In contrast, approach curves for both a native W/A interface (Figure

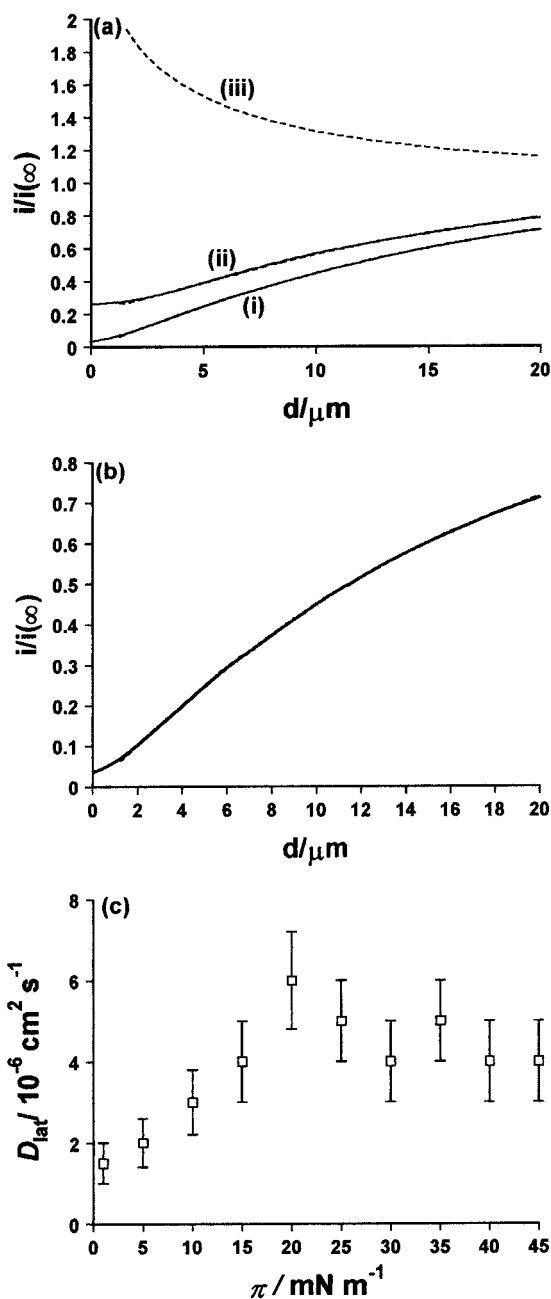


**Figure 4.** Typical approach curves for the measurement of lateral proton diffusion. (a) The solid experimental curves are for the reduction of  $0.5 \text{ mM H}_2\text{PO}_4^-$  at an UME approaching (i) a native W/A interface and (ii) a DPPS monolayer ( $\pi = 20 \text{ mN m}^{-1}$ ). The dashed curves are simulations for (i) an inert interface and (ii) the DPPS system with  $D_{\text{lat}} = 6 \times 10^{-6} \text{ cm}^2 \text{ s}^{-1}$  ( $A = 50 \text{ \AA}^2$ ) and (iii)  $D_{\text{lat}} = 1 \times 10^{-4} \text{ cm}^2 \text{ s}^{-1}$  ( $A = 50 \text{ \AA}^2$ ). (b) The six coincident solid experimental curves are for a DPPC monolayer ( $\pi = 1, 5, 10, 20, 30,$  and  $40 \text{ mN m}^{-1}$ ) and the dashed curve is the simulation for an inert interface. (c)  $D_{\text{lat}}$  as a function of surface pressure,  $\pi$ , derived from approach curve measurements for the DPPS system.

4a, (i)) and a DPPC monolayer (Figure 4b) showed a current response due only to the diffusion of  $\text{H}_2\text{PO}_4^-$  through solution.

For comparison, Figure 4a also shows the simulated behavior for the DPPS system when the lateral proton diffusion coefficient is comparable to the bulk proton diffusion coefficient. In this case, a significant increase in current is predicted as the UME approaches the monolayer that was not observed experimentally.

The approach curves in Figure 4b for DPPC at a wide range of surface pressures fit well to the simulation for an inert

(30) White, H. S.; Peterson, J. D.; Cui, Q. Z.; Stevenson, K. J. *J. Phys. Chem. B* **1998**, *102*, 2930.

(31) Bard, A. J.; Faulkner, L. R. *Electrochemical Methods: Fundamentals and Applications*; John Wiley & Sons: New York, 2001.

(32) Cevc, G.; Watts, A.; Marsh, D. *Biochemistry* **1981**, *20*, 4955.

(33) Heberle, J.; Dencher, N. A. *Proc. Natl. Acad. Sci. U.S.A.* **1992**, *89*, 5996.

(34) Unwin, P. R.; Bard, A. J. *J. Phys. Chem.* **1992**, *96*, 5035.

(35) Zhang, J. Ph.D. Thesis. University of Warwick, 2001.



interface. This suggests that the lateral proton flux at DPPC monolayers is insignificant. These results also demonstrate that a tip–interface separation of less than 2  $\mu\text{m}$  can readily be obtained with high reproducibility, in agreement with previous SECM measurements at different types of interface.<sup>14a,16,17,36</sup>

Lateral proton diffusion coefficients at DPPS derived from approach curve measurements are summarized in Figure 4c. As the surface pressure increased from 1 to 20 mN/m, the lateral proton diffusion coefficient,  $D_{\text{lat}}$ , increased from ca.  $1.5 \times 10^{-6} \text{ cm}^2 \text{ s}^{-1}$  to  $6 \times 10^{-6} \text{ cm}^2 \text{ s}^{-1}$ . At the higher pressures, where  $A$  changed only slightly (Figure 2), the lateral diffusion coefficient was reasonably uniform. These results clearly demonstrate that lateral proton diffusion occurs in acidic DPPS assemblies, but the diffusion coefficient is much smaller than the proton diffusion coefficient in bulk solution ( $8 \times 10^{-5} \text{ cm}^2 \text{ s}^{-1}$ ).<sup>9</sup>

These are the first quantitative data for proton diffusion in monolayers over a wide range of surface pressures. It is interesting that the lateral diffusion coefficients measured at DPPS in the liquid-condensed phase are lower than estimated for phospholipids in the liquid-expanded state;<sup>3,10,11b</sup> the latter phase has been proposed as a requirement for rapid lateral proton diffusion.<sup>11c</sup> The values measured herein, however, are of the same order of magnitude reported for proton diffusion at the purple membrane.<sup>7,13a</sup> The results in this paper clearly demon-

strate that the acid–base character of the phospholipid is important in determining the significance of interfacial proton transport. Furthermore, a large lateral diffusion coefficient is not a prerequisite for the observation of interfacial proton fluxes.

## Conclusions

A new SECM proton feedback approach has been developed for measuring lateral proton diffusion at phospholipid assemblies. Studies of monolayers of acidic DPPS (liquid-condensed phase) at a range of surface pressures suggest that lateral proton fluxes are significant, but the lateral proton diffusion coefficient is lower than in bulk solution. In contrast, the interfacial proton flux at zwitterionic DPPC (in both the liquid-expanded and liquid-condensed phases) cannot be detected with the SECM technique, suggesting that such effects are considerably smaller. The demonstration that the feedback mode can be operated with proton transfer, as well as electron transfer, opens up the possibility of utilizing SECM more widely to study interfacial proton-transfer dynamics with high spatial resolution.

**Acknowledgment.** We thank the BBSRC and EPSRC for support. J.Z. also gratefully acknowledges scholarships from the ORS scheme, the University of Warwick, and Avecia. Helpful discussions with Dr. C. J. Slevin are much appreciated.

(36) Shao, Y.; Mirkin, M. V.; Rusling, J. F. *J. Phys. Chem. B* **1997**, *101*, 3202.

JA012074W